Electronic Supplementary Information

Increased Disulfide Peptide Sequence Coverage via "Cleavage ON/OFF" Switch during Nanoelectrospray

*Gongyu Li, Yue Yin, and Guangming Huang**

Detailed Experimental Settings.

Table S1. Partial oxygen addition fragment ions observed in InESI-CID-MS analysis and sequence coverage for selectin binding peptide and somatostatin.

Scheme S1. Possible oxidative cleavage reaction pathway for the cleavage of DSB via radical generation in InESI.

Fig. S1. MS spectrum of the oxidative cleavage products from selectin binding peptide by InESI.

Fig. S2. MS^3 spectra of the oxidative cleavage products from selectin binding peptide by InESI.

Fig. S3. The increase trend of GSH, a pair-product of GSO• from DSB oxidative cleavage, with the increase of amplitude of the pulsed high voltage (1 kHz). Corona discharge and DSB cleavage was observed with a similar increase trend with adjusting of the amplitude of pulsed high voltage.

Fig. S4. Dependence of DSB dissociation on the frequency of pulsed high voltage (6 kV). In all these experiments, NH_4OAc (5 mM) was added into the spray solution.

Fig. S5. a) Comparison of oxidative cleavage reaction products from GSSG via InESI with different spray voltages and different electrolytes. Dependence of DSB dissociation on low concentration volatile electrolyte and amplitude of pulsed high voltage, as illustrated by b) GSO• and c) GSH. Different concentrations of NH_4OAc were indicated.

Fig. S6. a) Sonic spray ionization MS spectrum of GSSG in the presence of various concentrations of NH_4OAc. b) Magnification of a) for mass range between m/z 290 and 420. No oxidative cleavage reaction cleavage products (GSH, *m/z* 308 or GSO•, *m/z* 323) were observed in sonic spray ionization for the absence of corona discharge.

Fig. S7. Tandem MS spectrum (low m/z range) of $[M+5H]^{5+}$ for human insulin containing 10 mM NH_4OAc derived from "OFF" mode. Sequence information beyond the disulfide bonds were obtained.

Fig. S8. Reaction MS^1 spectrum of insulin and isotopic distributions of $^{O}Bb_7^{+}$ and $^{H}By_{20}^{2+}$ in InESI-CID-MS spectrum of HO• additive precursor ion ($[M + 5H + OH]^{5\bullet+}$, *m/z* 1166) of human insulin. It should be noted that the m/z 1166.0 in MS spectrum of insulin would be assumed to be NH_4^{+} adduction product. We excluded this possibility to some extent via CID tandem mass spectrometry and finally affirmed the possibility of radical additive ion.

Detailed Experimental Settings.

For nanoESI:

The size of spray emitter was kept 5-10 μm. The emitters were pulled from borosilicate glass capillaries (1.2 mm o.d., 0.9 mm i.d.) by using a P-2000 laser-based micropipette puller (Sutter Instruments, Novato, CA, USA). Spray voltage for nanoESI was optimized and specified for each experiment but was in the range of 1.0-2.0 kV dc. Tip to MS inlet was kept 5 mm for all nanoESI operations. Spray solvent was also optimized and H_2O was used as solvent if not specified.

For InESI:

For InESI, induced voltage was typically 4.0-12.0 kV_{p-p}, 1 kHz, duty cycle 50%, pulsed high voltage. This pulsed high voltage was originally generated from a 25 MHz function waveform generator (DG1022U, RIGOL, Beijing, China) and was then amplified by a household stereo power amplifier. As a result, 100 V_{p-p} pulsed voltage was obtained and followed a coil to further amplify the amplitude up to a final value of 0-20 kV_{p-p}. The high voltage was monitored with a digital oscilloscope (DS1052E, RIGOL, Beijing, China) after attenuating (1: 1000) with a attenuation rod. For the consideration of security and effectiveness of radical generation, 4-12 kV_{p-p} (1 kHz) was selected in our experiments. Other operation parameters for InESI were kept the same with nanoESI.

For MS:

All experiments were carried out with a LTQ-Velos Pro (Thermo Fisher Scientific, CA, USA) mass spectrometer equipped with an linear ion trap. MS inlet capillary temperature was kept 275 °C. Positive mode was operated for all cleavage identification experiments with S-lens value of 42%. CID energy was optimized to obtain considerable fragment ions and 15% was finally used if not specified (Insulin, 27%). Maximum injection time of ion trap was set as 10 ms for small peptides and 500 ms for insulin radical ion fragmentation to obtain acceptable MS^2 signal, and all are with 3 microscans. Isolation width was set as 1.0.

"Cleavage ON/OFF" experiment:

Cleavage ON/OFF tests were exemplified with GSSG (8 μM, 10 mM NH_4OAc) and insulin (34.4 μM, 50 mM NH_4OAc). For "Cleavage ON" mode was operated as follows, pulsed high voltage (1 kHz, 7 kV) was applied on the ring electrode outside the tip for InESI operation and DC high voltage for conventional nanoESI was meanwhile turned off. For "Cleavage OFF" mode, DC high voltage (1 kV) was applied on the electrode inside the nanotip for nanoESI operation and pulsed high voltage for InESI was meanwhile turned off. In order to avoid possible electric field interfere from induced voltage, nanoESI electrode was withdrawed when operating "Cleavage ON" mode.

Table S1. Partial oxygen addition fragment ions observed in InESI-CID-MS analysis and sequence coverage for selectin binding peptide and somatostatin.

Peptide	Partial oxygen addition fragment ions observed, *m/z*								Sequence Coverage
selectin binding peptide	$^{O}b_4^+$	$^{O}y_4^+$	$^{O}b_5^+$	$^{O}y_5^+$	$^{O}y_6^+$	$^{O}b_7^+$	$^{O}y_7^+$	$^{O}b_8^+$	
	474	492	587	605	718.5	786	847.5	942.5	
somatostatin	$^{O}y_7^+$	$^{O}b_8^+$	$^{O}y_8^+$	$^{O}b_9^+$	$^{O}y_9^+$	$^{O}b_{10}^+$	$^{O}y_{10}^+$	$^{O}b_{11}^+$	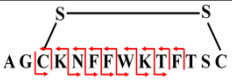
	888	970	1035	1098	1182	1199	1296	1346.6	

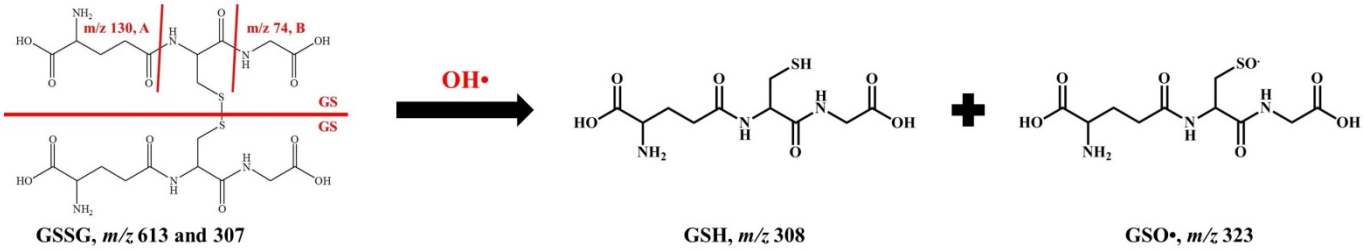

Scheme S1. Possible oxidative cleavage reaction pathway for the cleavage of DSB via radical generation in InESI.

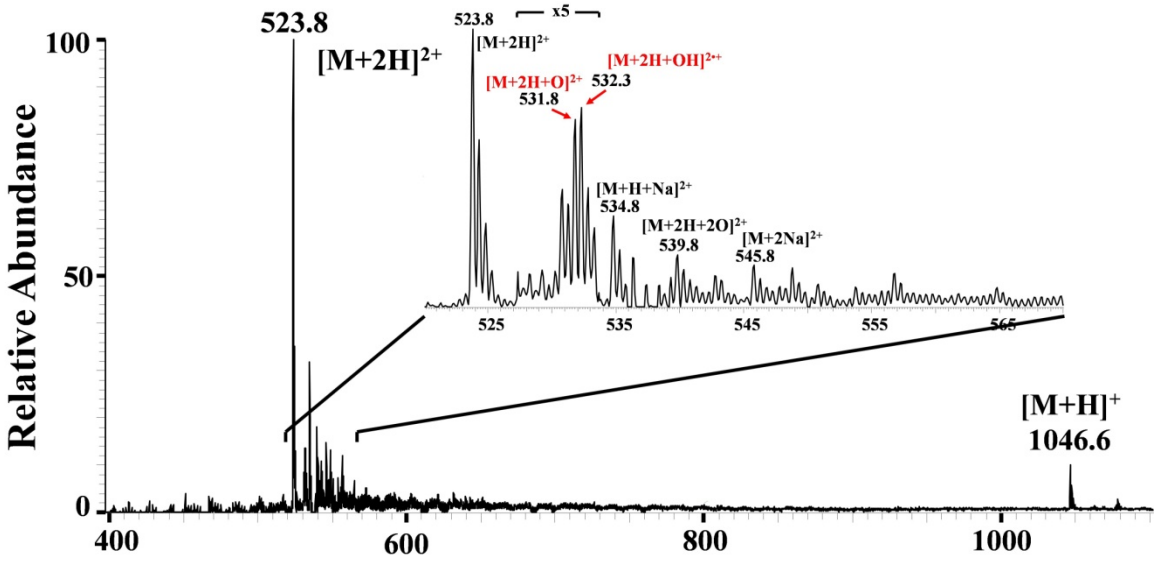

Fig. S1. MS spectrum of the oxidative cleavage products from selectin binding peptide by InESI.

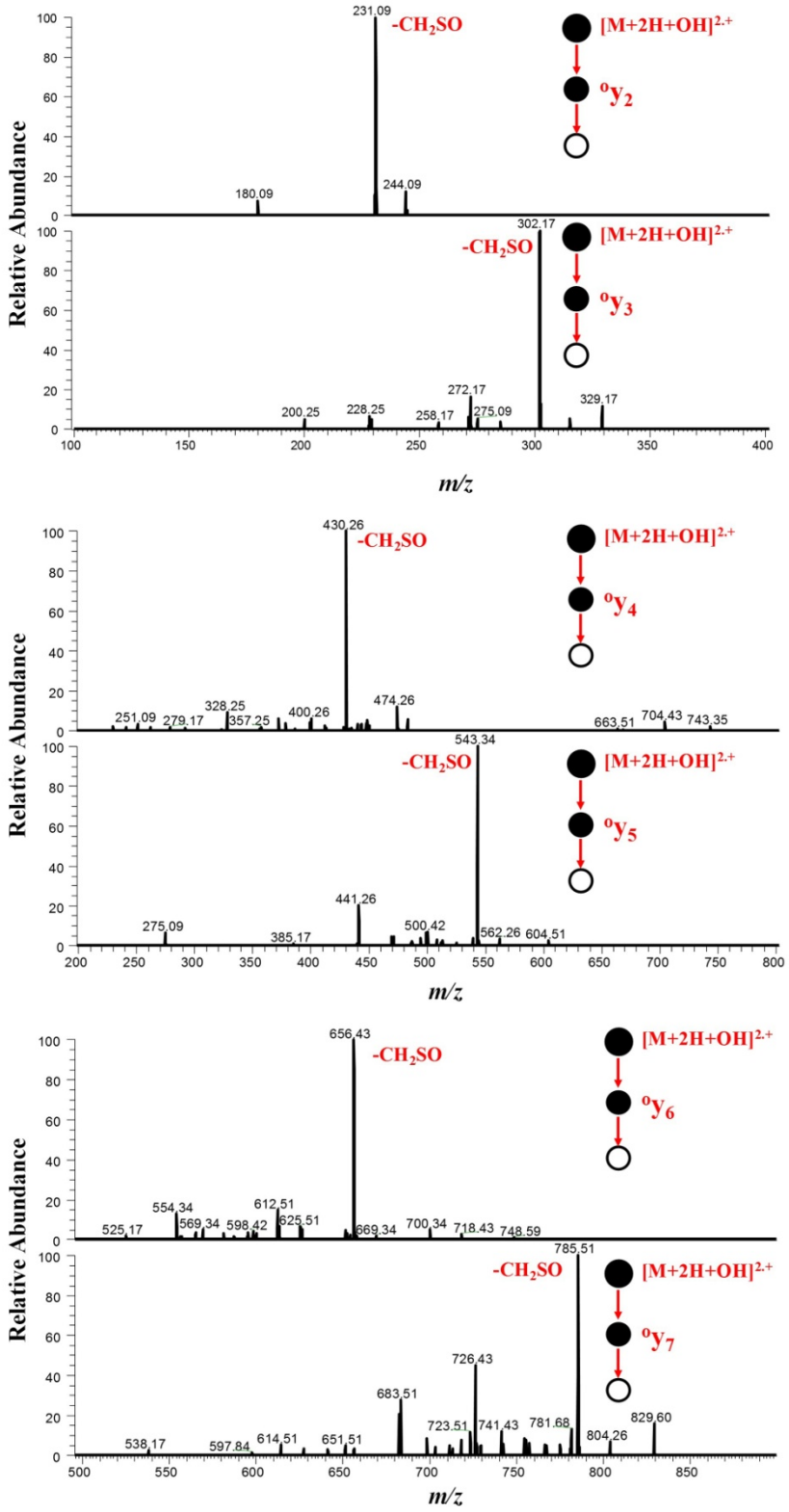

Fig. S2. MS^3 spectra of the oxidative cleavage products from selectin binding peptide by InESI.

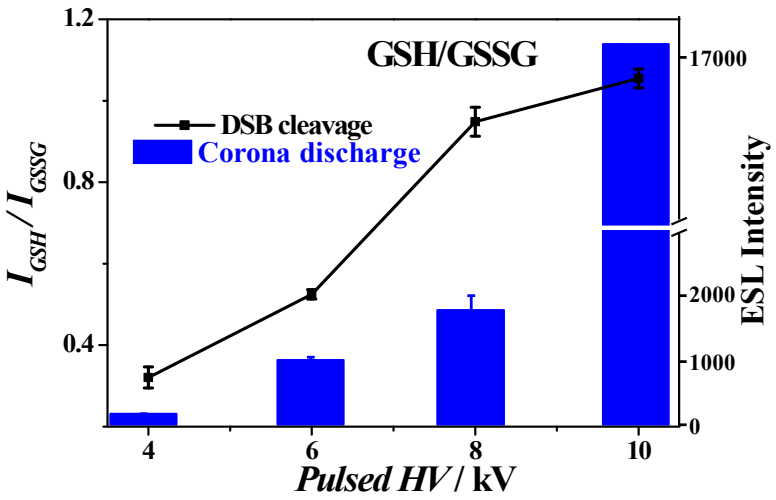

Fig. S3. The increase trend of GSH, a pair-product of GSO• from DSB oxidative cleavage, with the increase of amplitude of the pulsed high voltage (1 kHz). Corona discharge and DSB cleavage was observed with a similar increase trend with adjusting of the amplitude of pulsed high voltage.

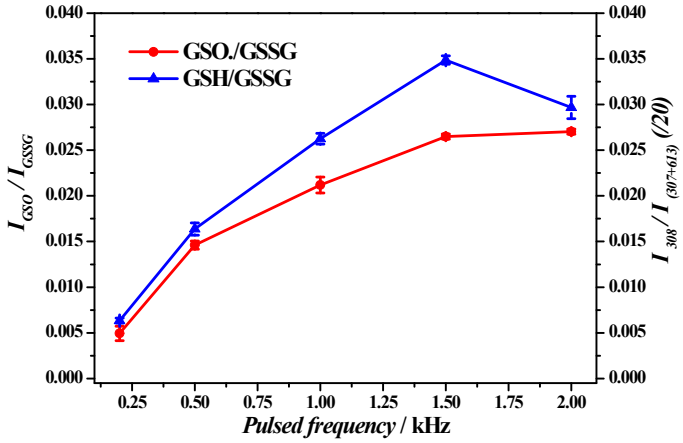

Fig. S4. Dependence of DSB dissociation on the frequency of pulsed high voltage (6 kV). In all these experiments, NH_4OAc (5 mM) was added into the spray solution.

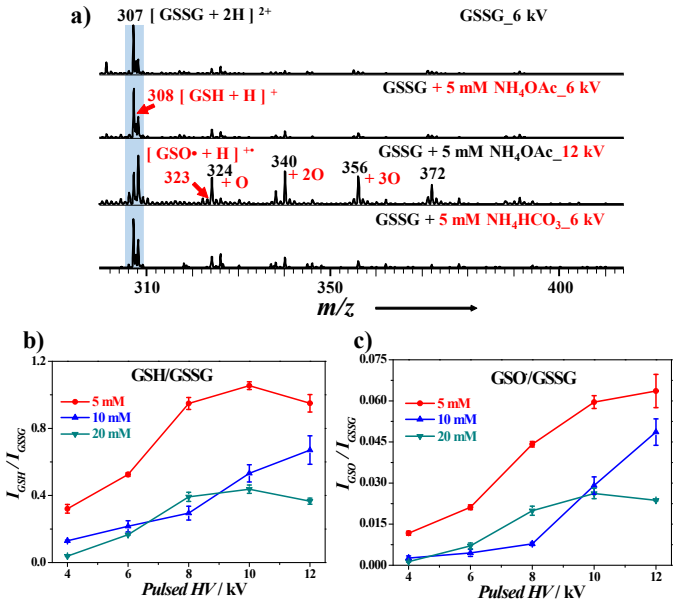

Fig. S5. a) Comparison of oxidative cleavage reaction products from GSSG via InESI with different spray voltages and different electrolytes. Dependence of DSB dissociation on low concentration volatile electrolyte and amplitude of pulsed high voltage, as illustrated by b) GSO• and c) GSH. Different concentrations of NH_4OAc were indicated.

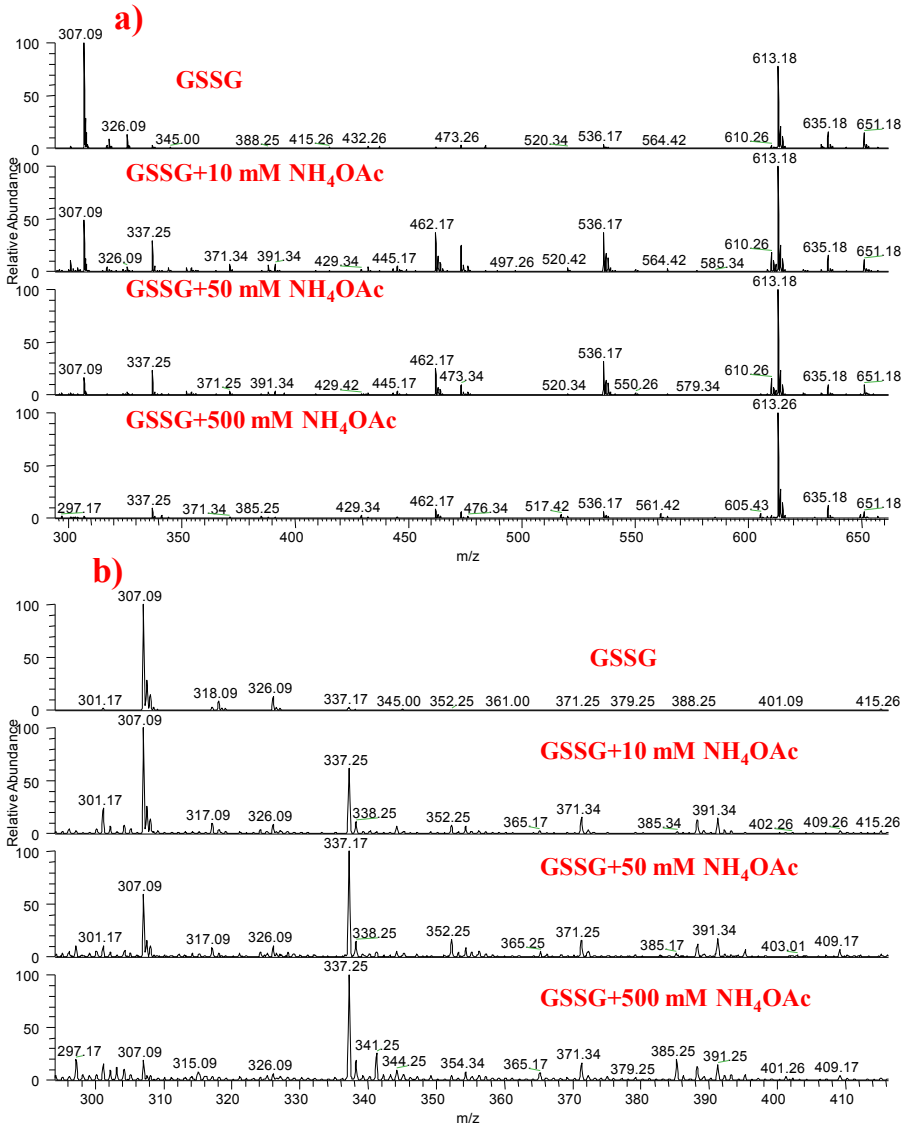

Fig. S6. a) Sonic spray ionization MS spectrum of GSSG in the presence of various concentrations of NH_4OAc. b) Magnification of a) for mass range between m/z 290 and 420. No oxidative cleavage reaction cleavage products (GSH, *m/z* 308 or GSO•, *m/z* 323) were observed in sonic spray ionization for the absence of corona discharge.

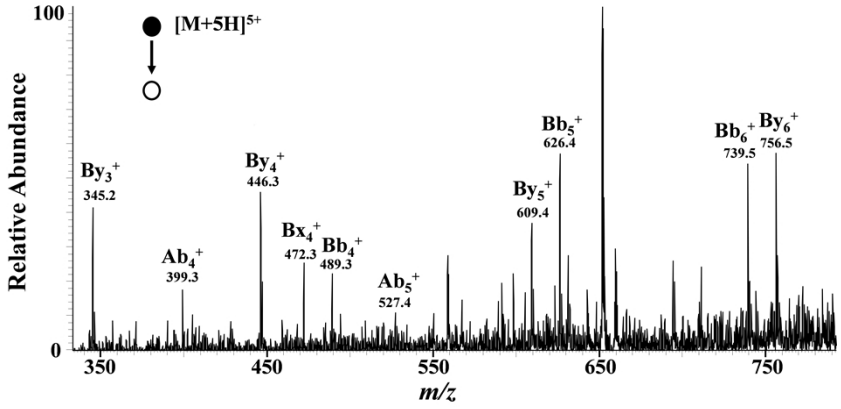

Fig. S7. Tandem MS spectrum (low m/z range) of $[M+5H]^{5+}$ for human insulin containing 10 mM NH_4OAc derived from "OFF" mode. Sequence information beyond the disulfide bonds were obtained.

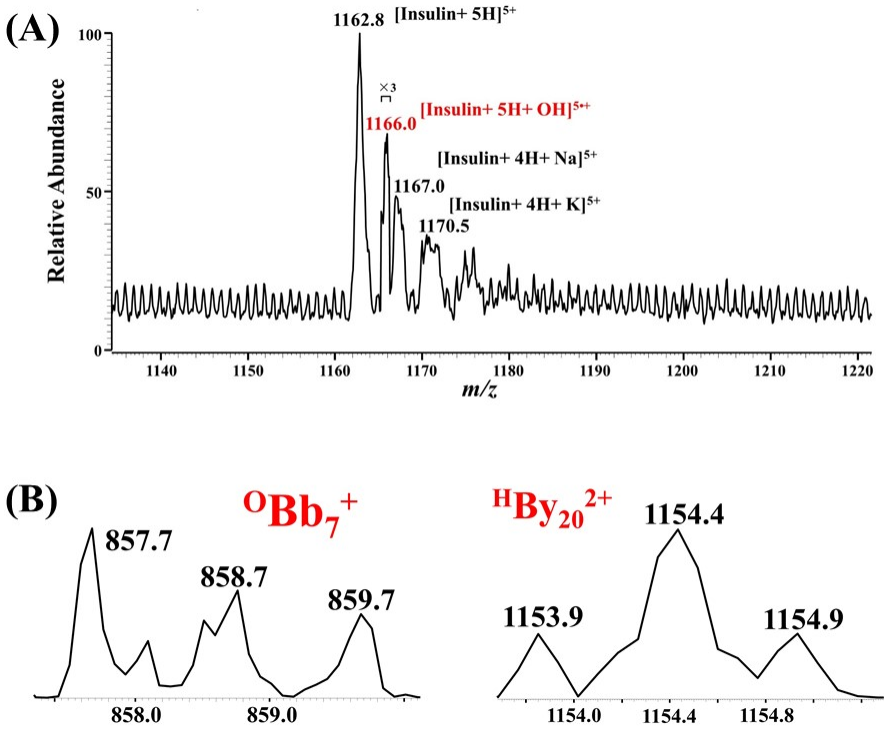

Fig. S8. Reaction MS^1 spectrum of insulin and isotopic distributions of $^{O}Bb_7^+$ and $^{H}By_{20}^{2+}$ in InESI-CID-MS spectrum of HO• additive precursor ion ($[M + 5H + OH]^{5\bullet+}$, *m/z* 1166) of human insulin. It should be noted that the m/z 1166.0 in MS spectrum of insulin would be assumed to be NH_4^+ adduction product. We excluded this possibility to some extent via CID tandem mass spectrometry and finally affirmed the possibility of radical additive ion.